Published in final edited form as:
*Chem Res Toxicol*. 2012 January 13; 25(1): 130–139. doi:10.1021/tx200333g.

# ARISTOLOCHIC ACID I METABOLISM IN THE ISOLATED PERFUSED RAT KIDNEY

**Horacio A. Priestap**[†,*], **M. Cecilia Torres**[‡], **Robert A. Rieger**[‡], **Kathleen G. Dickman**[‡], **Tomoko Freshwater**[§], **David R. Taft**[§], **Manuel A. Barbieri**[†], and **Charles R. Iden**[‡]

[†]Department of Biological Sciences, Florida International University, Miami, Florida, 33199

[‡]Department of Pharmacological Sciences, Stony Brook University, Stony Brook, NY 11794-3400

[§]Division of Pharmaceutical Sciences, Long Island University, Brooklyn, NY 11201-8423

## Abstract

Aristolochic acids are natural nitro-compounds found globally in the plant genus A*ristolochia* that have been implicated in the severe illness in humans termed aristolochic acid nephropathy (AAN). Aristolochic acids undergo nitroreduction, among other metabolic reactions, and active intermediates arise that are carcinogenic. Previous experiments with rats showed that aristolochic acid I (AA-I), after oral administration or injection, is subjected to detoxication reactions to give aristolochic acid Ia, aristolactam Ia, aristolactam I and their glucuronide and sulfate conjugates that can be found in urine and faeces. Results obtained with whole rats do not clearly define the role of liver and kidney in such metabolic transformation. In this study, in order to determine the specific role of the kidney on the renal disposition of AA-I and to study the biotransformations suffered by AA-I in this organ, isolated kidneys of rats were perfused with AA-I. AA-I and metabolite concentrations were determined in perfusates and urines using HPLC procedures. The isolated perfused rat kidney model showed that AA-I distributes rapidly and extensively in kidney tissues by uptake from the peritubular capillaries and the tubules. It was also established that the kidney is able to metabolize AA-I into aristolochic acid Ia, aristolochic acid Ia O-sulfate, aristolactam Ia, aristolactam I and aristolactam Ia O-glucuronide. Rapid demethylation and sulfation of AA-I in the kidney generate aristolochic acid Ia and its sulfate conjugate that are voided to the urine. Reduction reactions to give the aristolactam metabolites occur to a slower rate. Renal clearances showed that filtered AA-I is reabsorbed at the tubules whereas the metabolites are secreted. The unconjugated metabolites produced in the renal tissues are transported to both urine and perfusate whereas the conjugated metabolites are almost exclusively secreted to the urine.

## INTRODUCTION

Aristolochic acids are naturally occurring polyaromatic, nitro-compounds usually found in *Aristolochia* plants. Aristolochic acid I (AA-I) (**1**) or simply aristolochic acid (8-methoxy-6-nitro-phenanthro[3,4-d]-1,3-dioxole-5-carboxylic acid or 3,4-methylenedioxy-8-methoxy-10-nitro-1-phenanthrenecarboxylic acid) is found as the major component in the

**Corresponding Author**, Phone: 305-348-0375. Fax: 305-348-1986. horacio@pharm.stonybrook.edu.

ASSOCIATED CONTENT

s Supporting information. HPLC profiles of urine of isolated rat kidney perfused with AA-I and of urine of rat injected with AA-I under fluorescence and UV detection are shown in Figure 1. MS and MS/MS spectra of aristolochic acid Ia, aristolactam I, aristolactam Ia, aristolactam Ia O-glucuronide, aristolactam Ia O-sulfate and aristolochic acid Ia O-sulfate are given in Figure 2. Collision induced fragmentation pathways of the positive ammonium adduct of aristolochic acid Ia O-sulfate are shown in Scheme 2. This material is available free of charge via the Internet at http://pubs.acs.org.

mixture of AAs contained in the plants. It is usually accompanied by aristolochic acid II (AA-II) (6-nitro-phenanthro[3,4-d]-1,3-dioxole-5-carboxylic acid or 3,4-methylenedioxy-10-nitro-1-phenanthrenecarboxylic acid) found in somewhat lesser amounts. Serious adverse effects have been reported in humans after ingestion of herbal remedies containing AAs. The most remarkable ailment is the so-called Chinese herbs nephropathy (CHN), a unique type of progressive, renal fibrosis associated with the prolonged intake of Chinese herbs.[1] The observed nephrotoxicity was attributed to the intake of *Aristolochia fangchi* inadvertently included in slimming pills distributed at a Belgian weight loss clinic.[2] Also, a similar endemic nephropathy (BEN) was recognized in the Balkan region, and it has been suggested that ingestion of bread prepared with wheat grains contaminated with seeds of *Aristolochia clematitis* during harvesting is the cause of this ailment.[3]

Aristolochic acids are known to cause cancer in both animals and humans. After administration of AAs to rats, either orally or by injection, tumors were formed at several locations including the forestomach, stomach, kidney, lung and uterus.[4] In humans who have been exposed to AAs through herbs or other means, urothelial cancer is most prevalent.[5] Deoxyguanosine and deoxyadenosine adducts have also been found in human kidney and urothelial tissues.[6] Both AA-I and AA-II are genotoxic mutagens forming DNA adducts after metabolic activation. It was postulated that after partial reduction of the nitro group of AA-I and AA-II, an N-hydroxylactam is formed; the latter then yields a reactive nitrenium ion which binds to DNA.[7,8] Recently, an alternative mechanism of AA activation have been proposed[9] (subjects related to the mechanism of AA-activation are discussed in Reference 9).

Knowledge of the diverse biotransformations of aristolochic acids is necessary to understand the mechanisms involved in AA nephropathy and carcinogenicity in humans. Metabolic studies performed *in vivo* by administration of AA-I and AA-II to rats led to the identification of a number of AA-metabolites including demethylation, reduction, hydroxylation and denitration products, as well as their glucuronide, sulfate and acetyl conjugates.[10–12] By oral administration or injection of AA-I to rats metabolites such as aristolochic acid Ia (AA-Ia) (**2**), aristolactam I (L-I) (**3**), aristolactam Ia (L-Ia) (**4**), and the phase II metabolites aristolochic acid Ia O-sulfate (AA-Ia-O-S) (**5**), aristolactam Ia O-glucuronide (L-Ia-O-G) (**6**) and aristolactam Ia O-sulfate (L-Ia-O-S) (**7**) (Scheme 1) are usually encountered in urine and feces. Kidney and liver are known to play an important role in drug metabolism but their impact on the metabolism of AA-I is not clearly defined when working with whole animals. The kidney is an excretory organ for drugs and chemicals and their metabolic products, and also plays a role in the biotransformation of xenobiotics. The isolated perfused kidney (IPK) technique has become a useful research tool in drug disposition studies.[13] In order to assess the involvement of the kidney on the metabolism of AA-I (**1**), as well as the mechanisms of renal handling of AA-I (**1**) and the metabolites, isolated kidney experiments were performed in which AA-I was perfused. It is important to understand the function of the kidney on the biotransfomations suffered by AA-I since its toxic effects are attributable to metabolic conversion to reactive electrophilic intermediates, which, on reaction with cellular nucleophiles, lead to a variety of deleterious effects. This interaction between reactive intermediates and critical cellular macromolecules is intimately involved in the mutagenic changes observed in humans exposed to AAs. The identification of the enzymes involved in the activation of AAs and knowledge of their catalytic specificities is of paramount importance to understand the molecular mechanisms of AA-mediated renal injury and the different individual susceptibilities observed in humans exposed to AAs.[14,15] In vitro studies showed that the main human and rat enzymes activating AA-I are NAD(P)H:quinone oxidoreductase (NQO1), cytochrome P450 (CYP)

1A1/2, NADPH:CYP reductase (POR) and protaglandin H synthase (COX).[14] NQO1 is the most important enzyme responsible for AA-I activation in humans.[15]

In this study designed to explore the mechanisms involved in AA nephropathy and carcinogenesis, the metabolism of AA-I was examined in the isolated rat kidney and by subcutaneously injecting AA-I into rats. Preliminary data on the identification of AA-I-metabolites in rat urine were presented.[11–12] The metabolites of AA-I recovered during the metabolic studies were characterized by using chromatographic methods and mass spectrometer analysis. Since most of the phase I and phase II metabolites reported for AA-I and AA-II were not isolated and their identification relies almost exclusively on MS measurements, we report here our own mass spectral data and interpretations that may be useful for identification purposes [preliminary data on AA-I-metabolism and the identification of AA-I-metabolites in rat urine obtained in our laboratories were presented at the 53th and 54th American Society for Mass Spectrometry Conferences on Mass Spectrometry; Torres, M. C. et al., Aristolochic acid metabolism in the Rat, San Antonio, Texas, June 5–9, 2005 (WP 035); Rieger, R. A. et al., MS/MS characterization of new sulfate metabolites from aristolochic acid, Seatle, WA, May 28-June 1, 2006 (TP 028); and at the American Society of Nephrology, Annual Renal Week Meeting, 2005, Dickman, K. et al., Excretion of the nephrotoxin aristolochic acid I involves secretion of a demethylation product formed by intrarenal metabolism, J. Am. Soc. Nephrology, 16: 571A, 2005; see also Dickman, K. et al., Metabolism and transport of aristolochic acid by the rat kidney, Collegium Antropologicum (Zagreb, Croatia), 30, Suppl. 1 (2006) ]

## MATERIALS AND METHODS

**Caution:** *Aristolochic acid I is mutagenic in bacteria and tumorigenic in mammals. Therefore, appropiate safety procedures must be followed when working with this compound.*

### Materials

Samples of AA-I (**1**), L-I (**3**) and L-Ia (**4**) from plant origin[16] were used as standards. Before use, AA-I was purified by preparative HPLC and recrystallization from dioxane to >98 % purity. β-Glucuronidase and arylsuphatase (Type H-I Helix pomatia) and ammonium acetate were obtained from Sigma (St. Louis, MO). HPLC-grade acetonitrile, methanol and triethylamine required for the HPLC buffer were purchased from Fisher Scientific. Pure water (18.2 MΩ) was produced by a Milli-Q Ultrapure water system.

### IPK Experiments

Experiments with isolated perfused kidney were conducted with Sprague-Dawley rats according to the method previously described by Taft.[15] Two kidneys denoted as A and B were obtained from two male rats. Following kidney excision and transfer to the recirculating perfusion system, the organ was allowed to stabilize for 10 minutes. An aliquot (27 μL) of a stock solution of AA-I in DMSO (50 mg/mL) was added as a bolus dose to the recirculating perfusate (80 mL) to reach an initial perfusate concentration of ca. 50 μM. Perfusate was sampled 5 min post-dose and every 10 min thereafter. The perfusate volume was mantained at 80 ml during the experiment by addition of fresh perfusate. Urine was collected in 10-min intervals over the entire experiment (80 min). The volume of urine collected per 10-min interval was average 0.756 ml (S.D. 0.126) and 0.742 ml (S.D. 0.133) for kidneys A and B, respectively (Table 2).

The amounts of AA-I and the metabolites in the perfusate of kidney A at 10–20, 20–30, 30–40, 40–50, 50–60, 60–70 and 70–80 min periods were obtained from the analytically

determined concentrations in perfusate (samples taken at 15, 25, 35, 45, 55, 65 and 75 min of the experiment) and the perfusate volumes (80 ml at all periods). Amounts of AA-I and metabolites in the urines for each 10-min period were obtained from the analytically determined concentrations in urine and the corresponding urine volumes (average 0.765 ml for 10-min period). Concentrations of AA-I and metabolites at the 70–80 min period are shown in Table 3.

The amounts of AA-I and the metabolites in the perfusate and urines of kidney A were determined as indicated above. The following average amounts of AA-I and metabolites in perfusate and urines of kidney A at 40–50. 50–60, 60–70 and 70–80 min periods were found (the average amount corresponds to a 10-min period): perfusate, nanomoles (S.D. in parenthesis), AA-I (**1**), 1441 (139); AA-Ia (**2**), 71.6 (31.0); L-I (**3**), 0.086 (0.062); L-Ia (**4**), 0.97 (0.52); urine: AA-I (**1**), 0.36 (0.05); AA-Ia (**2**), 0.72 (0.11); L-I (**3**), 0.029 (0.013); L-Ia (**4**), 0.10 (0.03); AA-Ia-O-S (**5**), 0.36 (0.05); L-Ia-O-G (**6**), 0.019 (0.007).

The amounts of AA-I and the metabolites recorded for kidney B at each period was determined as indicated above. The following average amounts of AA-I and metabolites in perfusate and urines of kidney B at 40–50. 50–60, 60–70 and 70–80 min periods were found (the average amount corresponds to a 10-min period): perfusate, nanomoles (S.D. in parenthesis), AA-I (**1**), 2447 (298); AA-Ia (**2**), 38 (10); L-I (**3**), 0.35 (0.05); L-Ia (**4**), 0.29 (0.09); urine: AA-I (**1**), 1.24 (0.32); AA-Ia (**2**), 6.7 (2.6); L-I (**3**), 0.034 (0.015); L-Ia (**4**), 0.089 (0.071); AA-Ia-O-S (**5**), 0.96 (0.28); L-Ia-O-G (**6**), 0.012 (0.009).

## Viability parameters

Parameters were monitored to assess kidney function during the experiments. The following viability parameters were monitored for each urine collection period (S.D. in parenthesis): urine flow rate (UFR), 0.075 (0.013) mL/min; urine pH, 6.97 (0.14); glomerular filtration rate (GFR) (estimated as inulin clearance), 0.65 (0.06) mL/min; fractional reabsorption (FR) of glucose, 0.98 (0.00); $FR_{Na}$, 0.91 (0.01); $FR_{K}$, 0.48 (0.07); $FR_{Cl}$, 0.88 (0.02). Perfusion pressure was maintained at 100 +/− 10 mmHg by adjusting perfusion flow rate as necessary.

## Data analysis

Parameters were determined by standard methods.[17–18] The area under the perfusate concentration time curve (AUC) for AA-I was calculated using the trapezoidal rule. Briefly, a plot of concentrations of AA-I in the pefusate (Cp, μmoles/mL), recorded at 15, 25, 35, 45, 55, 65 and 75 min of the experiment, versus time was constructed. The most probable curve was traced. The AUC was determined as follows. Eight trapeziums were constructed under the curve at 0–10 min, 10–20 min, etc. (until 80 min). The approximate area of each trapezium was calculated as usual, e.g., by multiplying the average concentration (Cp) by the trapezium width (10 min). The $AUC_{0–80}$ (μmoles × min/mL), representing the area under the curve over the period of sample collection post-dose, was found by adding the calculated areas of the eight trapezoids. The cumulative AA-I excretion in the urine (Xu) is the total amount of AA-I excreted to the urine during the eight periods (0–80 min) (2.5 μmoles and 6.5 μmoles for kidneys A and B, respectively). Renal clearance ($CL_R$) of AA-I expressed in mL/min was calculated as the ratio of the cumulative excretion (Xu) and AUC (0–80 min) over the duration of the sampling period, i.e. Xu/ $AUC_{0–80}$ (calculated $CL_R$ values were 0.0014 and 0.0030 mL/min for kidneys A and B respectively; Table 2). Filtration clearance ($CL_{FILT}$) was defined as the product of glomerular filtration rate (GFR) and the fraction unbound to albumin in perfusate ($f_u$).[17] The perfusate binding of AA-I (and the metabolites) was determined by ultrafiltration as previously described[17] ($f_u$ values of 0.0225, 0.0220 and 0.0235 were determined for AA-I (**1**), AA-Ia (**2**) and L-I (**3**), respectively). The excretion ratio (XR) was calculated as the ratio of $CL_R$ and $CL_{FILT}$.

Estimates of XR greater than 1 indicate net tubular secretion whereas values less than 1 indicate net tubular reabsorption.[15] The XR values determined for AA-I with the AUC method and other renal excretion parameters for AA-I are shown in Table 2.

The renal clearances of AA-I, as well as those of the metabolites, were also independently calculated for the 10–20, 20–30, 30–40, 40–50, 50–60, 60–70 and 70–80 min periods of the IPK experiment from the concentration in urine (Cu), concentration in perfusate (Cp), urine flow rate (UFR) and glomerular filtration rate (GFR) which were separately recorded for each period. The renal clearance (Cl) for AA-I and the metabolites for each time period was calculated as Cl = Cu × UFR/Cp. Subsequently, the renal excretion ratio (XR) was calculated as $XR = Cl/ f_u \times GFR$. Seven different XR values, one for each period, were obtained for AA-I and the metabolites. The average XR values for AA-I and the metabolites are given in Table 4.

## In Vivo Experiments with rats

Five male Wistar rats weighing 250–300 g were housed separately in metabolic cages for urine and feces collection. Two mg (6.7–8 mg/Kg) of AA-I dissolved in DMSO (20 μL) was subcutaneously injected into the rats. Urine was collected during 24 hours after injection of AA-I and stored at −80 °C. The average volume of urine collected (24 hours) was 34.8 mL (S.D. 8.8). The following average concentrations (μg/Lt) of AA-I and the metabolites for 24-hour collected urines were found (standard deviation in parentheses): AA-I (**1**), 68 (17); AA-Ia (**2**), 7900 (1300); L-I (**3**), 5.4 (3.8); L-Ia (**4**), 1600 (678); L-Ia-O-G (**6**), 66 (54); L-Ia-O-S (**7**), 53 (24). μM average concentrations of AA-I and metabolites are given in Table 3.

## Sample preparation

Urine and perfusate samples collected during in vivo experiments with rats and IPK experiments were stored at −80 °C prior to analysis. Exactly measured 200–500 μL aliquots of urine, depending of the amount available, were transferred to centrifugal tubes, and four volumes of methanol were added. The samples were then shaken and allowed to stand for half an hour. After centrifugation at 14000 rpm for 20 min, the supernatants were removed and dried under *vacuo* at room temperature in a Savant vacuum centrifuge. The residues were dissolved in exactly measured 100–200 μL of DMSO, centrifuged, and 20–50 μL was analyzed by HPLC.

## HPLC Analysis

The Waters HPLC system (Milford, MA) consisted of a 600 E Multisolvent Delivery System, a U6K injector, and a Waters 996 Photodiode Array Detector (PDA); a Waters Model 2475 Fluorescence Detector was connected downstream of the UV detector. Data were acquired and analyzed using the Waters Empower software. The chromatograph was fitted with a 25 cm × 4.6 mm i.d. reverse phase X-Terra $C_{18}$ MS column used at room temperature. Chromatograms and peak areas were based on UV detection at 254 nm; UV spectra were collected between 200 and 500 nm. The wavelengths utilized by the fluorescence detector were 390 nm for excitation and 480 nm for emission [under present HPLC detection conditions the fluorescence emission by L-I (**3**) largely exceeds that of L-Ia (**4**)]. The mobile phase consisted of (A) 0.1 M triethyl ammonium acetate buffer (prepared with acetic acid and freshly distilled triethyl amine, adjusted to pH 7.5, and filtered) and (B) acetonitrile. The column was eluted at 1.2 mL/min with 20 to 30% B over 30 min followed by 30 to 75% B in 10 min, then maintaining 75% B for 10 min. Finally, the mobile phase was programmed for a brief wash with 100% B and a return to the initial conditions for a period of 20 min for reconditioning prior to the next injection. Both solvents were degassed with helium during analysis. Collected fractions were dried in a Savant vacuum centrifuge

prior to ESI-MS and MS-MS analysis. Occasionally, the metabolites in the collected fractions were further purified by re-chromatography in the same system.

### ESI-MS and ESI-MS-MS Analysis

All experiments were performed on a Micromass Quattro LCZ mass spectrometer (Waters, Beverly, MA). The instrument was fitted with a nanospray ion source for nano electrospray ionization (nano-ESI). The source was operated in the positive and negative ion mode at 80° C. Collected fractions or standards were dissolved in 10 μL of 50% acetonitrile / 2.5 mM Ammonium acetate or 50% acetonitrile /water and 3 μL was transferred to a New Objective PicoTip (Woburn, MA). The filled tip was mounted in the nanospray source and 800 volts was applied to initiate nano-ESI. The emitter voltage and cone voltage were optimized to produce intense signal, and a positive ion survey scan (*m/z* 300–1200) was taken. Then MS/MS spectra were acquired in the range *m/z* 50–500 on each protonated molecular ion or ammonium adduct ion observed in the survey scan. Subsequently, a negative ion survey scan was acquired, and a similar approach was employed to obtain negative ion MS/MS data on the deprotonated molecular ions observed. MS/MS data were collected in the profile mode (multi-channel analysis) and processed upon the completion of the run.

Matrix assisted laser desorption ionization - time of flight (MALDI-TOF) analyses were performed on a *Voyager-DE STR* mass spectrometer system (Applied Biosystems, Framingham, Massachusetts) operated in the reflector mode. Samples were dissolved in a 50% solution of acetonitrile/0.1% TFA in water containing ∝-cyano-4-hydroxy cinammic acid (5mg/ml) and dried on the sample plate. The accelerating voltage was set to 20 kV. The mass scale (*m/z* 400–5000) was calibrated with a mixture of peptides.

## RESULTS AND DISCUSSION

The metabolites identified in urine and feces of rats after administration of AA-I are the result of general metabolic mechanisms used by the organism to rapidly and safely eliminate toxic substances. However, not all metabolites are nontoxic or even less toxic than the parent molecule, and some may be sufficiently reactive to chemically modify macromolecules in the cell. Pathways for biotransformation of AA-I in mammals are shown in Scheme 1. The kidney is the primary organ responsible for the excretion of foreign compounds and their biotransformation products, and it is the target organ for AAs. The mechanisms of renal excretion and metabolism of drugs by the kidney have been reviewed.[19–21] The isolated perfused kidney (IPK) methodology is one of the most valuable tools for studying renal excretion mechanisms.[15] Results of our metabolic studies performed *in vivo* by administration of AA-I to the isolated kidney as well as whole rats are summarized below.

### Isolated Perfused Kidney Experiments

Two experiments were conducted to define the disposition of AA-I (**1**) and its metabolites in the isolated perfused kidney. These experiments were performed with kidneys of two Sprague-Dawley rats denoted as Rat A and Rat B. Results are shown an Tables 2–4. Collected urines and samples of perfusate were analyzed by HPLC, ESI/MS and ESI/MS/MS (Table 1). Differences were found between the kidneys of the two animals. For example, AA-I was more rapidly absorbed from perfusate by kidney A than by kidney B. Also, it was found that with kidney B the concentrations of the metabolite AA-Ia (**2**) were higher in the urine and lower in the perfusate as compared to those of kidney A. The cause of this different behavior is not known since glomerular filtration rate, fractional reabsorption of $Na^+$ and glucose, and other viability parameters (see Experimental Section) were normal and stable over 80 min, indicating the absence of malfunction or toxicity.

The AA-I-perfused kidney (50 μM AA-I in 80 ml of perfusate) excreted mainly AA-Ia, both free (**2**) and as the sulfate conjugate (**5**) (Supporting Information, Figure 1A). The minor metabolites L-I (**3**), L-Ia (**4**) and L-Ia-O-G (**6**) were observed only by fluorescence detection.

During the experiment perfusate concentrations of AA-I progressively dropped from ca. 28 μM (sample taken at 15 min) to ca. 16 (Rat A) or 23 (Rat B) μM (at 75 min), whereas more or less constant values of 0.5 (Rat A) or 1.2 (Rat B) μM were recorded for the concentrations of AA-I in the urines collected during the last periods. Results suggest that AA-I was little metabolized during the experiment (total metabolites recorded were <3% of the dose at 80 min). Binding to circulating albumin ($f_u$ 2.2 %) would affect the filtration rate of AA-I. The renal excretion parameters for AA-I are shown in Table 2 and Table 4. The excretion ratio (XR) estimates of AA-I are consistent with net tubular re-absorption of filtered AA-I. Both low filtration rate and tubular re-absorption would substantially reduce the urinary recovery of intact AA-I. Lack of precision in the calculated renal parameters is expected because complications such as eventual passage of albumin into the glomerular filtrate[22] were left out of consideration in this study.

The IPK technique allows for estimation of the amount of xenobiotic accumulated in the kidney. At the end of the experiment (80 min), amounts of AA-I in perfusate and urines accounted for less than 50 % of the dose. Since during this period the production of metabolites was only incipient (<3% of the dose), it may be assumed that, as observed in other systems,[17,23] AA-I can distribute rapidly and extensively in this organ (Table 2). Calculations show that AA-I absorption and storage in the kidney would be carried out mostly by uptake from peritubular capillaries rather than by reabsortive uptake from the tubular filtrate. Accumulation of AA-I in kidney is important in connection to its harmful effects since it was reported that AA may directly cause the acute renal toxicity and apoptosis responsible for interstitial nephropathy through regulating mitochondrial transition permeability.[24]

AA-Ia (**2**) was found to be the main metabolite of AA-I in both urine and perfusate (Table 3). Within a few minutes after the onset of the experiment, AA-Ia (**2**) and its sulfate conjugate (**5**) were detected in the urine in an approximate ratio 3:1 (Supplementary Information, Figure 1A). Concentrations of AA-Ia (**2**) in the urines promptly attained more or less constant values of ca. 1 and 7 μM for rats A and B at 30–80 min. Significant amounts of AA-Ia (**2**) accumulate in the perfusate. In contrast, AA-Ia-O-S (**5**) could not be identified in the perfusate.

The reduced metabolites were produced at a slower rate. L-Ia (**4**) could be detected in the urine only after 20 min and L-Ia-O-G (**6**) after 30–40 min of AA-I administration. The small amount of L-Ia-O-G (**6**) produced was almost entirely secreted to the urine. L-I (**3**) appeared rapidly in the urine (10 min) but its levels in urine and perfusate remained low throughout the experiment.

It should be noted that the amounts of metabolites in perfusate largely exceed those secreted into the urine. The total amount of metabolites recorded in the urines scarcely account for 0.1–0.2 % of the dose. On the other hand, the total amount of metabolites found in perfusate increases to about 2.5 % of the dose at the end of the experiment (80 min). Despite dispersal of experimental data and differences between both kidneys, the metabolites invariably showed excretion ratios (XR) well above 1 at all periods indicating net secretion at the tubules (Table 4). Calculations also indicate that the metabolites produced in the kidney would be much more efficiently transported and voided to the capillaries than to the tubules.

The concentrations of AA-I-metabolites rapidly increase in perfusate and urines during the first periods of the IPK experiments (10–20, 20–30 and 30–40 min). Between 40 and 80 min of the experiment, the levels of metabolites in perfusate and urines increase at a slower rate

The above results show that kidney cells can efficiently demethylate absorbed AA-I to yield AA-Ia (**2**). Conjugation with sulfuric acid to yield AA-Ia-O-S (**5**) is also a rapid reaction. In contrast, the late secretion of L-Ia (**4**), the low levels of L-I (**3**) and the high AA-Ia/L-Ia ratio in both urine and perfusate throughout the entire IPK experiment suggest that reduction is a relatively slow process as compared with demethylation in the rat kidney.

## Metabolism of AA-I in rat

After subcutaneous injection of 2 mg AA-I into Wistar rats, 24 hr urine samples were collected, extracted and analyzed by HPLC, ESI/MS and ESI/MS/MS (Table 1). This protocol led to the identification of five AA-I metabolites, namely AA-Ia (**2**), L-I (**3**), L-Ia (**4**), L-Ia-O-G (**6**) and Ia-O-S (**7**). Consistent with IPK experiments, AA-Ia (**2**) was found to be the most abundant metabolite excreted to the urine by the rat (Supporting Information, Figure 1C). L-Ia (**4**) was also excreted in significant amounts. HPLC with florescence detection revealed three minor metabolites, L-I (**3**), L-Ia-O-S (**7**) and L-Ia-O-G (**6**) (Supporting Information, Figure 1B). The metabolites AA-Ia-O-S (**5**) and 3,4-methylenedioxy-8-hydroxy-1-phenanthrene-1-carboxylic acid (**9**) were also present, but at such low concentrations that they could only occasionally be observed by UV detection. The average concentrations of each metabolite found in the urine samples is shown in Table 3. The total amount of metabolites in the 24 hr urine sample would represent ca. 18% of the dose (AA-Ia (**2**), 14.3 %; L-I (**3**), 0.01 %; L-Ia (**4**), 3.4 %; L-Ia-O-G (**6**), 0.09 %; L-Ia-O-S (**7**), 0.09 %).

AA-Ia (**2**) and L-Ia (**4**) in unconjugated form largely predominate in the urine extracts of AA-I-injected rats. AA-Ia (**2**) can stem from demethylation of AA-I in both liver and kidney. However, most of L-Ia (**4**) found in the rat urine may arise from demethylation and reduction of AA-I in liver since the isolated kidney excretes L-Ia (**4**) at a slow rate. The same may be true for L-Ia-O-G (6) and L-Ia-O-S (**7**). The collected rat urines only contain AA-Ia-O-S (**5**) in trace amounts. It is to be noted that metabolites may also be excreted via bile, be modified in gut and reabsorbed or secreted in feces.[10,25]

Interestingly, Krumbiegel *et al*. found L-Ia (**4**) to be the main metabolite in male Wistar rat urine, but in such experiments (orally administered AA-I) most of L-Ia (**4**) was encountered in conjugated forms [presumably as L-Ia-O-G (**6**) and L-Ia-O-S (**7**)].[10] The above discrepancies suggest that the final pattern of metabolites found in urine may be highly dependent upon the genetic attributes of the rat and/or the mode of administration of AA-I.

## Metabolism of AA-I in Kidney and Liver

Humans are differently affected when exposed to AAs. Different individual susceptibility to AAs may be due to variations in the activity of enzymes catalyzing activation/detoxification of AAs and the regulatory proteins controlling expression of these enzymes.[15,26] Understanding which human enzymes are involved in activation and detoxication of AAs, and knowledge of their genetic polymorphisms and catalitic specificity, is important in the assessment of individual susceptibility to these plant toxins. The major hepatic and renal enzymes responsible for DNA adduct formation in humans have been characterized.[27] AAs are activated by nitroreduction. Phase I enzymes that reductively activate AAs play a crucial role in AA-DNA adduct formation. *In vitro* studies showed that the main human and rat enzymes activating AA-I are NAD(P)H:quinone oxidoreductase (NQO1), present in hepatic and renal cytosolic subcellular fractions, and cytochrome P450 (CYP) 1A1/2 which occur in

liver microsomes.[27] Also important are NADPH:CYP reductase (POR) in kidney microsomes and protaglandin H synthase (cyclooxygenase, COX) in urothelial tissues.[27] While most of the enzymes catalyzing the reductive activation of AA-I *in vitro* have been identified, it is not clear which of them actually participates in this process *in vivo*. A recent study established that NQO1 is the most important enzyme responsible for AA-I activation in humans.[15] NQO1 could be induced in AAN and BEN patients, which might led to an increased risk to the carcinogen.[15]

The enzymes that demethylate AA-I (**1**) to AA-Ia (**2**) may play an important role in detoxication of AA-I because AA-Ia (**2**) has only a limited toxicity.[28] Consequently, rapid and efficient demethylation of AA-I may protect the kidney from the carcinogenic and nephrotoxic effects produced by AA-I. Demethylation of AA-I is catalyzed by CYP enzymes.[15,26–32] It was established that CYP1A1 and CYP1A2 are the most active of 18 human P450s tested in demethylating AA-I.[30] The adverse effects caused by AA-I and the different inter-individual susceptibility to this toxin may be determined by the relative activity of reducing enzymes such as NQO1, catalyzing AA-DNA adduct formation, and demethylating enzymes, which convert AA-I (**1**) into the nontoxic AA-Ia (**2**).[26,28,29,30] Studies with *Cyp1a2*-null mice support this view. *Cyp1a2*-null mice are more sensitive to AA-I-elicited nephrotoxicity and accumulate AA-DNA adducts at a higher rate than control mice.[30] Consequently, AA-I demethylation, mediated by Cyp1A2 is a primary pathway of AA-I detoxication.[28,30]

The IPK studies show that the rat kidney is able to metabolize AA-I into AA-Ia (**2**), AA-Ia-O-S (**5**), L-I (**3**), L-Ia (**4**) and L-Ia-O-G (**6**). The kidney demethylates AA-I to AA-Ia (**2**) which is partially conjugated with sulfuric acid to yield AA-Ia-O-S (**5**), these detoxication reactions accounting for the predominant secretion of AA-Ia (**2**) and AA-Ia-O-S (**5**) in the urines collected during IPK experiments (Table 3). Studies in mice have shown that hepatic cytochrome P450 1A1 and 1A2 detoxicate AA-I (**1**) by demethylation to give the nontoxic derivative AA-Ia (**2**).[29,30] The studies here described indicate that the isolated kidney of rat is also quite efficient in demethylating AA-I. The urine of the isolated kidney perfused with AA-I mainly contain AA-Ia (**2**), free or conjugated as sulfate. This implies that demethylation in kidney is more efficient than nitroreduction and that renal CYP1A1 and CYP1A2 may contribute to detoxification of AA-I-administered rats by metabolizing AA-I into less toxic metabolites. NQO1, CPR and COX are the major enzymes involved in reduction of AA-I (**1**) and AA-Ia (**2**) into L-I (**3**) and L-Ia (**4**) in kidney.[27] The kidney is also provided with sulfotransferases which transfer a sulfate group to AA-Ia (**2**) to produce AA-Ia-O-S (**5**).

The basis for the selective renal toxic effects of AAs, which specifically targets the proximal tubule, has not been established, but may involve metabolic and/or transport mediated processes. It was recently shown that organic ion transporters (OATs) 1 and 3 mediate concentrative uptake of AA-I (**1**) in the mouse proximal tubule and may be involved in the site-selective toxicity of this nephrotoxin.[31] Thus, in the IPK, OATs 1/3 likely mediate basolateral uptake of AA-I (**1**) from the perfusate. The nephrotoxin then undergoes demethylation or nitroreduction in the proximal tubule, followed by secretory efflux of metabolites to the urine and/or reabsortive efflux of metabolites to the perfusate.

The liver is known to be the main site of biotransformation and conjugation of xenobiotics. Previous studies suggest that AA metabolism occurs primarily in the liver.[29,30] The absence or low levels of AA-Ia-O-S (**5**) and the increased formation of L-Ia (**4**) with respect to AA-Ia (**2**) observed in the urine of the rat, support the liver as predominantly responsible for AA-I-metabolism. Also, the relatively increased amount of L-Ia (**4**) in the urine of rat probably reflects a more efficient reduction of AA-Ia (**2**) in the liver. As stated above, the most

important human and rat enzymes activating and detoxicating AA-I in liver are NQO1, CYP1A1 and CYP1A2.[15,27,29,30]

AAs can undergo metabolic activation affording carcinogenic species that can bind to DNA and induce malignant transformations.[8,26] Nitroreduction is the major pathway responsible for the carcinogenic changes induced by AAs. It has been suggested that the liver, as a tissue rich in biotransformation enzymes, can produce toxic AA-metabolites that can be transported to the kidney through the systemic circulation and cause kidney toxicity (directly or via further metabolism).[26,29] While this hypothesis remains to be demonstrated by further investigations, the *in vivo* studies here described show that the rat kidney is provided with the enzymes necessary to reduce AA-I (**1**) to L-I (**3**) and, consequently, to generate *in situ* the reactive intermediates involved in AA-DNA adduct formation. NQO1, POR, COX are the principal enzymes reductively activating AA-I in kidney and could be responsible for AA-DNA adduct formation in kidney of humans exposed to AAs.[27,32] The cause of renal failure as well as the molecular mechanisms of AA-mediated renal injury and urothelial tumor development are still a matter of debate.[27]

## Characterization and mass spectral properties of the AA-I metabolites

**Aristolochic acid Ia (AA-Ia) (2)—**The ionization characteristics of AA-I (**1**) and AA-II have been previously reported for ESI and APCI ionization methods.[33] AAs have a strong affinity for ammonium ions and are, therefore, optimally detected as $[M+NH_4]^+$ adduct ions in the positive ion mode.[33] Some mass spectral properties of AA-I (**1**) and AA-Ia (**2**) observed in this study are given in Table I. The fragmentation pattern AA-Ia (**2**) closely resembles that of AA-I (**1**). Using positive ion ESI, AA-Ia (**2**) easily generates the $[M+NH_4]^+$ adduct ion. When subjected to collision induced dissociation (CID) on a triple quadrupole mass spectrometer, the AA-Ia ammoniated ion (m/z 345) initially undergoes loss of $NH_3$ to give the protonated molecular ion $[M+H]^+$ followed by the loss of one of three neutral molecules: $H_2O$, $CO_2$ or $NO_2$ (Table 1; Supporting Information, Figure 2A). The base peak is *m/z* 284 $[(M+NH_4)\text{-}NH_3\text{-}CO_2]^+$.

**Aristolactam I (3) and aristolactam Ia (4)—**Under EI-MS aristolactams are known to suffer successive losses of neutral fragments ($CH_3$, CO, $H_2CO$, HCN) from the substituents attached to the phenanthrene ring e.g., fragment ions observed at m/z 278, 250, 220, 192, 164 and 137 for L-I (**3**) suggest successive losses of $CH_3$, CO, H2CO, CO, CO and CNH from the molecular ion (m/z 293). In LC/MS with positive ESI mode, aristolactams produce a protonated molecular ion. The CID mass spectrum of these ions for L-I (**3**) and L-Ia (**4**) are summarized in Table I. Interestingly, the protonated molecular ion of both aristolactams shows a more complex fragmentation pattern (Supporting Information; Figures 2B and 2C) than that for the analogous ammoniated acids (Supporting Information, Figure 2A). The MS/MS spectra of the protonated ions of aristolactams show successive losses of neutral fragments. Inspection of the positive ESI/MS/MS spectrum of L-Ia (Supporting Information; Figure 2C) shows significant peaks at m/z 222, 195, 167, and 137 that may result from successive losses of $H_2CO$, CO, CNH, CO and $H_2CO$ from the protonated molecular ion ($[M+H]^+$, m/z 280). Similarly, peaks at m/z 206, 178, 151 suggest degradation via loss of $H_2O$, 3CO, and CNH. When a methoxy group is present in the molecule, as in the case of L-I (**3**), loss of a methyl radical followed by loss of CO are the most important primary fissions (Table 1; Supporting Information; Figure 2B).

**Sulfate Conjugate of AA-Ia (5)—**AA-Ia-O-S (**5**), $C_{16}H_9NO_{10}S$, MW 407, is an important metabolite that gives an intense peak at *m/z* 425, $(M+NH_4)^+$ in the positive ESI mode and at *m/z* 406, $(M\text{-}H)^-$ in the negative ESI mode (Supporting Information, Figure 2D). The daughter ions of ammoniated AA-Ia-O-S (m/z 425) (Supporting Information,

Figure 2E) can be interpreted as outlined in Scheme 2 (Supporting Information; the $[M+H]^+$ ion formed by loss of ammonia, m/z 408 $[(M+NH_4)\text{-}NH_3]^+$, appears at very low intensity possibly because of facile subsequent elimination of $CO_2$ and $H_2O$ to give the *m/z* 364 and 390 ions). The CID spectrum of both $(M+NH_4)^+$ and $(M\text{-}H)^-$ ions show loss of 80 Da ($SO_3$) indicating the presence of a sulfate ester in the molecule. The MS/MS spectra of the $(M\text{-}H)^-$ ion of AA-Ia-O-S (*m/z* 406) shows daughter ions at m/z 326, 280 and 235 due to successive losses of SO3, NO2 and COOH (Supporting Information, Figure 2F).

Generation of multiple ionization products from AAs, in part by losses of neutral fragments ($CO_2$, $H_2O$), under APCI and ES ionization conditions have been reported.[33] In the ESI mass spectrum of AA-Ia-O-S (**5**) in the negative ion mode, in addition to $[M\text{-}H]^-$ (*m/z* 406), fragment ions are also observed at m/z 428, 420, 361, 359 and 325 (Supporting Information, Figure 2D). Product ion analysis shows the following. The ion at *m/z* 361 seems to be the simple sulfate analog of 8-hydroxy-3,4-methylenedioxy-1-phenanthrenecarboxylic acid due to removal of $NO_2$ from the molecule of AA-Ia sulfate during ESI. MS/MS of this ion (Supporting Information, Figure 2G) shows main daughter ions at *m/z* 281 and 237 that can be attributed to losses of $SO_3$ and $CO_2$. On the other hand, the simple spectrum produced by the *m/z* 359 ion (Supporting Information, Figure 2H) reveals little information other than the loss of the $SO_3$ fragment. Thus, the *m/z* 359 ion could be formulated as the anion of the lactone Ia sulfate (360 Da) (Supporting Information, Figure 2H), the latter arising from AA-Ia-O-S by concerted removal of the nitro group and cyclization of the carboxylic group on position 10 of the phenanthrene skeleton. In addition, the minor peak at *m/z* 428 (Supporting Information, Figure 2D) can be thought as $[M\text{-}H\text{-}H+Na]^-$ ion and the peak at *m/z* 325 suggests the losses of two protons and $SO_3^-$ ($[M\text{-}H\text{-}H\text{-}SO_3]^-$) or one proton and the $SO_3H$ radical. The above observations show that significant fragmentation of the AA-Ia-O-S molecule occurred under ESI conditions. Losses of $CO_2$ and water, i.e. generation of the $[(M\text{-}H)\text{-}44]^-$ and $[(M\text{-}H)\text{-}18]^-$ ions, reported to occur when using APCI and ES,[33] were not very significant under our ESI(-) conditions.

The evidence discussed above and the occurrence of this sulfate conjugate as an immediate metabolite of AA-I (**1**), together with AA-Ia (**2**) in the urine of the isolated perfused kidney, (Supporting Information, Figure 1A) support the structure of an 8-hydroxy-3,4-methylenedioxy-10-nitro-1-phenanthrenecarboxylic acid O-sulfate (**5**).

**Sulfate conjugate of L-Ia (7)—**L-Ia-O-S, $C_{16}H_9NO_7S$, MW 359, was characterized from the urine of rats injected with AA-I. ESI/MS analysis in the negative ion mode of the HPLC fractions containing this conjugate afforded a intense peak at *m/z* 358, $[M\text{-}H]^-$. The MS/MS of this ion afforded a peak at *m/z* 278 (Supporting Information, Figure 2I), a loss of 80 Da from the molecular ion, indicating that this compound is a sulfate conjugate. This assignment was verified by treating the corresponding HPLC-fractions with arylsulfatase (Type H-I Helix Pomatia) affording the free L-Ia (**4**). MS data do not discern between an O- or N-sulfate; however, UV spectra proved to be helpful in this regard (see below).

**Glucuronide conjugate of L-Ia (6)—**L-Ia-O-G, $C_{22}H_{17}NO_{10}$, MW 455, is excreted in the urine of rats treated with AA-I. This compound was also identified in the urine of rats administered with a mixture of AA-I and AA-II by Chan et al.[12] ESI-MS analysis of HPLC fractions containing this compound produced ions at *m/z* 456, $[M+H]^+$, in the positive ion mode, and at *m/z* 454, $[M\text{-}H]^-$, in the negative ion mode. CID of *m/z* 454 afforded a simple MS/MS spectrum (Supporting Information, Figure 2J) that showed a typical loss of the glucuronic acid moiety (176 Da) to give the negative ion of the lactam at *m/z* 278. The peaks at *m/z* 175, 174 and 113 correspond to negative fragments derived from the rupture of the glucuronic acid moiety and were previously identified by Gu et al.[34] L-Ia glucuronide shows a UV spectrum similar to those of L-I and L-Ia, and HPLC fractions containing this

compound were hydrolyzed with β-glucuronidase to produce L-Ia. Consequently, this compound is a glucuronide conjugate of L-Ia, but neither UV nor CID spectra are able to differentiate between the possible O- or N-conjugates. The identity of this metabolite was determined by treatment with ethereal diazomethane followed by mass spectrometer analysis. Since the nitrogen in the lactam ring does not react with $CH_2N_2$ and the OH group in L-Ia (**4**) is known to be quantitatively methylated by $CH_2N_2$, either one or two methyl groups were expected to be introduced into the molecule for the O- or the N-conjugate, respectively. The reaction product failed to give ions by ESI, but an ion at *m/z* 470 was detected by MALDI-MS. The observed $(M+H)^+$ ion at *m/z* 470 is consistent with the introduction of a single methyl moiety into the molecule, giving the expected mass for the O-glucuronide. The N-glucuronide would have been methylated at two positions, the 8-hydroxy group and the glucuronic acid carboxyl group, giving an ion at *m/z* 484. Evidence that the carboxyl group of L-Ia-O-G was methylated was provided by the MS/MS analysis of the *m/z* 470 ion, which revealed a facile loss of 190 Da from the $[M+H]^+$ ion instead of the usual loss of 176 Da observed with glucuronide conjugates. The structure of 8-hydroxy-3,4-methylenedioxy-10-amino-1-phenanthrene-carboxylic acid lactam O-glucuronide, or aristolactam Ia O-glucuronide (**6**), is proposed for this compound.

**UV Spectra of AA-I metabolites—**AA-I (**1**), AA-Ia (**2**) and AA-I methyl ester afford practically the same UV spectrum (Table 1). However, a significant hypsochromic shift of the two long wavelength bands is observed in the UV spectrum of AA-Ia-O-S (**5**). Certainly, the UV spectrum of AA-Ia-O-S (**5**) is almost superimposable upon that of AA-II, which does not contain substituents on the ring C of the phananthrene nucleus. Hypsochromic shifts of long wavelength maxima were previously observed in acetylated phenols, e.g. O-cresyl acetate, which shows a return to the spectrum of toluene because (due to the presence of the electron attracting group) the lone pair of electrons on oxygen are not available for the electron transfer transition to the π-orbital of the ring.[35] Comparison of the UV spectra of AA-I (Table 1) and AA-II ($\lambda_{max}$ 251, 302 and 367 nm) shows that the oxygenated functions (OH, OMe) at C-8 contribute to the displacement and intensity of the long wavelength bands. This effect disappears in AA-Ia-O-S (**5**) because of the presence of the electron withdrawing $SO_3H$ moiety attached to the C-8 oxygen, and the molecule contains then the chromophore of AA-II.

When compared with the parent compounds L-I (**3**) and L-Ia (**4**), the UV spectrum of L-Ia sulfate (**7**) shows a remarkable hypsochromic shift of the two bands at longer wavelengths together with the appearance of fine structure. As a whole, the UV spectrum of L-Ia sulfate (Table 1) closely resembles that of L-II ($\lambda_{max}$ 262, 277, 288, 328, 342, 374, 393). Thus, L-Ia sulfate (**4**) shows the same UV absorption behavior previously observed with AA-Ia-O-S (**5**), which is consistent with the structure of an O-sulfate. These effects in the UV spectrum would not be expected for an N-sulfate. The nonbonding nitrogen electrons interact with the nucleus, and attachment of an electron withdrawing group, i.e. N-acetylation, causes a shift of the absorption bands.[36] The absorption maxima of the N-acetyl aristolactam I ($\lambda_{max}$ 241, 286, 327, 387, 406 nm) reveal a hypsochromic shift of the L-I bands at 230–300 nm, whereas the effect on the long wavelength bands is less significant. This is not the case with L-Ia sulfate suggesting that the NH group has not been perturbed. Thus, UV evidence strongly supports sulfation at the 8-OH, and the molecule is then proposed to be 8-hydroxy-3,4-methylenedioxy-10-amino-1-phenanthrenecarboxylic acid lactam O-sulfate or aristolactam Ia O-sulfate (**7**).

## CONCLUSIONS AND PERSPECTIVES

Because of the small quantities of biological fluids usually available for analyses and the low concentrations of the metabolites present, MS measurements are a particularly valuable

tool for detection and characterization of metabolic products of aristolochic acids. However, identification of metabolites in a complex matrix (without a previous fractionation) only based on mass spectral data may lead to erroneous conclusions. In this paper we have shown that ESI/MS and ESI-MS-MS analyses of aristolochic acid metabolites obtained as purified fractions from HPLC together with information from UV spectra, chemical reactions, and enzymatic hydrolysis may provide additional information for a more precise characterization of the metabolites. In the future studies on the role of reactive metabolites of AA-I on toxicity, we propose (1) to isolate active intermediate reduction products from AA-I which subsequently will be tested in *in vitro* and *in vivo* experiments with rats, and (2) structural modifications of the parent compound (AA-I) to determine the structural features required for toxicity and ADN-adducts formation.

## Supplementary Material

Refer to Web version on PubMed Central for supplementary material.

## Acknowledgments

We thank Dr. Shinya Shibutani (Department of Pharmacological Sciences, Stony Brook University, Stony Brook) for *in vivo* experiments with rats.

**Funding Sources**

This study was carried out at the Department of Pharmacological Sciences, Stony Brook University, Stony Brook, New York, and supported by a research grant from the National Institute of Environmental Health Sciences (ES-04068).

## ABBREVIATIONS

| | |
|---|---|
| **AAN** | aristolochic acid nephropathy |
| **BEN** | Balkan endemic nephropathy |
| **AA** | aristolochic acid |
| **AA-I** | aristolochic acid I |
| **AA-II** | aristolochic acid II |
| **AA-Ia** | aristolochic acid Ia |
| **AA-Ia-O-S** | aristolochic acid Ia O-sulfate |
| **L-I** | aristolactam I |
| **L-Ia** | aristolactam Ia |
| **L-II** | aristolactam II |
| **L-Ia-O-S** | aristolactam Ia O-sulfate |
| **L-Ia-O-G** | aristolactam Ia O-glucuronide |
| **G** | glucuronic acid |
| **IPK** | isolated perfused kidney |
| **EI** | electron ionization |
| **ES** | electro spray |
| **ESI** | electro spray ionization |

| | |
|---|---|
| **CID** | collision induced dissociation |
| **$f_u$** | fraction of metabolite unbound to albumin |
| **OAT** | organic anion transporter |
| **XR** | excretion ratio |

## REFERENCES


1. Vanherweghem J-L, Depierreux M, Tielemans C, Abramowicz D, Dratwa M, Jadoul M, Richard C, Vandervelde D, Verbeelen D, Vanhaelen-Fastre R, Vanhaelen M. Rapidly progressive interstitial renal fibrosis in young woman: association with slimming regimen including Chinese herbs. Lancet. 1993; 341:387–391. [PubMed: 8094166]
2. Vanhaelen M, Vanhaelen-Fastre R, But P, Vanherweghem J-L. Identification of aristolochic acid in Chinese herbs. Lancet. 1994; 343:174. [PubMed: 7904018]
3. Hranjec T, Kovac A, Kos J, Mao W, Chen JJ, Grollman AP, Jelakovic B. Endemic nephropathy: The case for chronic poisoning by. Aristolochia Croat. Med. J. 2005; 46:116–125.
4. Mengs U, Lang W, Poch JA. The carcinogenic action of aristolochic acid in rats. Arch. Toxicol. 1982; 51:107–119.
5. Nortier JL, Muniz M-C, Schmeiser HH, Arlt VM, Bieler CA, Petein M, Depierreux MF, de Pauw L, Abramowicz D, Vereerstraeten P, Vanherweghem J-L. Urothelial carcinoma associated with the use of Chinese herbs (*Aristolochia* species). N. Eng. J. Med. 2000; 342:1686–1692.
6. Schmeiser HH, Bieler CA, Wiessler M, van Ypersele de Strihou C, Cosyns JP. Detection of DNA adducts formed by aristolochic acid in renal tissue from patients with Chinese herbs nephropathy. Cancer. Res. 1996; 56:2025–2028. [PubMed: 8616845]
7. Pfau W, Schmeiser HH, Wiessler M. Aristolochic binds covalently to the exocyclic amino group of purine nucleotides in DNA. Carcinogenesis. 1990; 11:313–319. [PubMed: 2302759]
8. Arlt VM, Stiborova M, Schmeiser HH. Aristolochic acid as probable human cancer hazard in herbal remedies: a review. Mutagenesis. 2002; 17:265–277. [PubMed: 12110620]
9. Priestap HA, de los Santos C, Quirke JME. Identification of a Reduction Product of Aristolochic Acid: Implications for the metabolic activation of carcinogenic aristolochic acid. J. Nat. Prod. 2010; 73:1979–1986. [PubMed: 21141875]
10. Krumbiegel G, Hallensleben J, Mennicke WH, Rittmann N, Roth HJ. Studies on the metabolism of aristolochic acids I and II. Xenobiotica. 1987; 17:981–991. [PubMed: 3673113]
11. Chan W, Cui L, Xu G, Cai Z. Study of the phase I and phase II metabolism of nephrotoxin aristolochic acid by liquid chromatography/tandem mass spectrometry. Rapid Commun. Mass Spectrom. 2006; 20:1755–1760. [PubMed: 16676316]
12. Chan W, Luo H-B, Zheng Y, Cheng Y-K, Cai Z. Investigation of the metabolism and reductive activation of carcinogenic aristolochic acids in rats. Drug Metab. and Dispos. 2007; 35:866–874.
13. Taft DR. The Isolated perfused rat kidney model: A useful tool for drug discovery and development. Curr. Drug Discov. Technol. 2004; 1:97–111. [PubMed: 16472223]
14. Stiborova M, Frei E, Schmeiser HH. Biotransformation enzymes in development of renal injury and urothelial cancer caused by aristolochic acid. Kidney Int. 2008; 73:1209–1211. [PubMed: 18480852]
15. Stiborova M, Mares J, Frei E, Arlt, Martinek E, VM, Schmeiser HH. The human carcinogen aristolochic acid I is activated to form DNA adducts by human NAD(P)H:quinone oxidoreductase without the contribution of acetyltransferases or sulfotransferases. Environ. Mol. Mutagen. 2011; 52:448–459. [PubMed: 21370283]
16. Priestap HA. Seven aristololactams from *Aristolochia argentina*. Phytochemistry. 1985; 24:849–852.
17. Poola NR, Kalis M, Plakogiannis FM, Taft DR. Characterization of pentamidine excretion in the isolated rat kidney. J. Antimicrob. Chemother. 2003; 52:397–404. [PubMed: 12888599]

18. Ajavon AD, Bonate PL, Taft DR. Renal excretion of clofarabine: Assesment of dose-linearity and role of renal transport systems on drug excretion. Eur. J. Pharm. Sci. 2010; 40:209–216. [PubMed: 20347037]
19. Anders MW. Metabolism of drugs by the kidney. Kidney Int. 1980; 18:636–647. [PubMed: 7463957]
20. Besseghir K, Roch-Ramel F. Renal excretion of drugs and other xenobiotics. Renal Physiol., Basel. 1987; 10:221–241.
21. Lohr JW, Willsky GR, Acara MA. Renal drug metabolism. Pharm. Rev. 1998; 50:107–141. [PubMed: 9549760]
22. Maack T. Physiological evaluation of the isolated perfused rat kidney. Am. J. Physiol. 1980; 238:F71–F78. [PubMed: 6987899]
23. Shanahan KM, Evans AM, Nation RL. Disposition of morphine in the rat isolated perfused kidney: Concentration ranging studies. J. Pharmacol. Exp. Ther. 1997; 282:1518–1525. [PubMed: 9316867]
24. Qi X, Cai Y, Gong L, Liu L, Chen F, Xiao Y, Wu F, Li Y, Xue X, Ren J. Role of mitochondrial permeability transition in human renal tubular epithelial cell death induced by aristolochic acid. Toxicol. Applied Pharmacol. 2007; 222:105–110.
25. Horton TL, Pollack GM. Enterohepatic Recirculation and Renal Metabolism of Morphine in the Rat. J. Pharm. Sci. 1991; 80:1147–1152. [PubMed: 1815073]
26. Stiborova M, Frei E, Arlt VM, Schmeiser HH. Metabolic activation of carcinogenic aristolochic acid, a risk factor for Balkan endemic nephropathy. Mut. Res. 2008; 658:55–67. [PubMed: 17851120]
27. Stiborova M, Hudecek J, Frei E, Schmeiser HH. Contribution of biotransformation enzymes to the development of renal injury and urothelial cancer caused by aristolochic acid: Urgent questions, difficult answers. Interdisc. Toxicol. 2008; 1:8–12.
28. Shibutani S, Bonala RR, Rosenquist T, Rieger R, Suzuki N, Johnson F, Miller F, Grollman AP. Detoxification of aristolochic acid I by O-demethylation: less nephrotoxicity and genotoxycity of aristolochic acid Ia in rodents. Int. J. Cancer. 2010; 127:1021–1027. [PubMed: 20039324]
29. Xiao I, Ge M, Xue X, Wang C, Wang H, Wu X, Li L, Liu L, Qi X, Zhang Y, Li Y, Lou H, Xie T, Gu J, Ren G. Hepatic cytochrome P450s metabolize aristolochic acid and reduce its kidney toxicity. Kidney Inter. 2008; 73:1231–1239.
30. Rosenquist TA, Einolf HJ, Dickman KG, Wang L, Smith A, Grollman AP. Cytochrome P450 1A2 detoxicates aristolochic acid in the mouse. Drug Metab. Dispos. 2010; 38:761–768. [PubMed: 20164109]
31. Dickman KG, Sweet DH, Bonala R, Ray T, Wu A. Physiological and molecular characterization of aristolochic acid transport by the kidney. J. Pharmacol. Exp. Ther. 2011; 338:588–597. [PubMed: 21546538]
32. Stiborova M, Frei E, Hodek P, Wiessler M, Schmeiser HH. Human hepatic and renal microsomes, cytochromes P450 1A1/2, NADPH:cytochrome P450 reductase and prostaglandin H synthase mediate the formation of aristolochic acid-DNA adducts found in patients with urothelial cancer. Int. J. Cancer. 2005; 113:189–197. [PubMed: 15386410]
33. Kite GC, Yule MA, Leon C, Simmonds MSJ. Detecting aristolochic acids in herbal remedies by liquid chromatography/serial mass spectrometry. Rapid Commun. Mass Spectrom. 2002; 16:585–590. [PubMed: 11870896]
34. Gu J, Zhong D, Chen X. Analysis of O-glucuronide conjugates in urine by electrospray ion trap mass spectrometry. Freseniu J. Anal. Chem. 1999; 365:553–558.
35. Scott, AI. Oxford: Pergamon Press; 1964. Interpretation of the ultraviolet spectra of natural products; p. 91
36. Pit CG, Fowler MS. Electronic absorption spectra of aminosilanes. J. Am. Chem. Soc. 1967; 89:6792–6793.

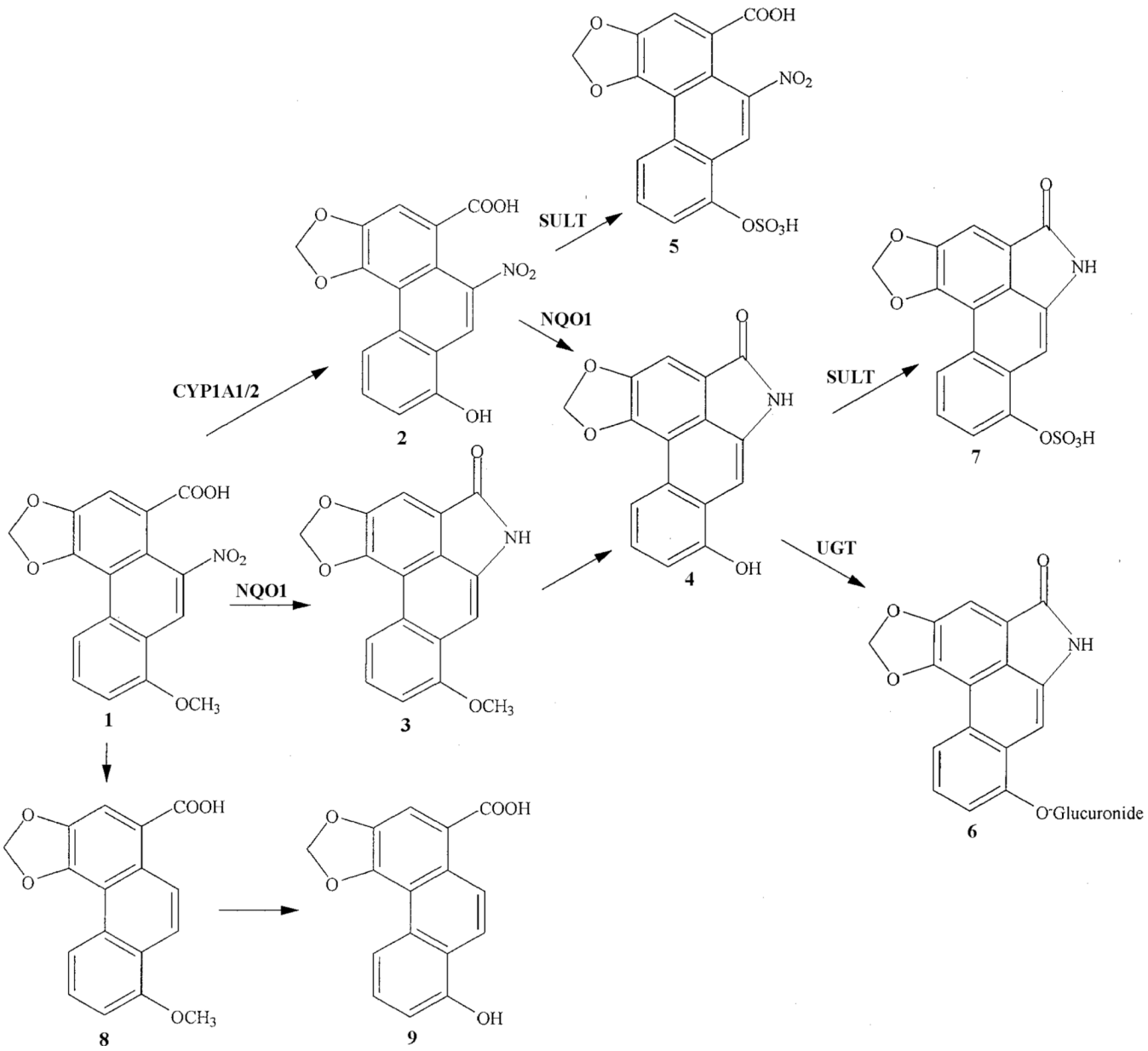


**Scheme 1.**

Metabolic pathways of AA-I in rats.

CYP1A1/2, cytochrome P450 1A1/2; NQO1, NAD(P)H:quinone oxidoreductase; SULT, sulphotransferase; UGT, UDP-glucuronyl transferase

**Table 1**

Retention times, UV $\lambda_{max}$ values and mass spectral characteristics of AA-I and its metabolites.

| | MW | Rt (min) | UV ( λmax.) | m/z ESI(+) | m/z ESI(−) |
|---|---|---|---|---|---|
| Aristolochic acid Ia O-sulfate (**5**) | 407 | 6.6 | 253, 308, 399 | 425 $[M+NH_4]^+$<br>$MS^2$ [425]: 407, 390, 364, 318, 310, 284, 237 (see Scheme 2) | 406 $[M-H]^-$, 361, 359<br>$MS^2$ [406]: 326 $[M-H-SO_3]^-$; 280 $[M-H-SO_3-NO_2]^-$; 235 $[M-H-SO_3-NO_2-CO_2H]^-$<br>$MS^2$ [361]: 281$[361-SO_3]^-$; 237 $[281-SO_3-CO_2]^-$<br>MS2 [359]: 279 $[359-SO_3]^-$ |
| Aristolactam Ia O-glucuronide (**6**) | 455 | 7.7 | 237, 262, 294, 332, 398 | 456 $[M+H]^+$ | 454 $[M-H]^-$<br>$MS^2$ [454]: 278 $[M-H-176]^-$; 175 $[G]^-$; 174 $[G]^-$ |
| Aristolochic acid Ia (**2**) | 327 | 9.2 | 252, 317, 369 | 345 $[M+NH_4]^+$; 655 $[2M+H]^+$<br>$MS^2$ [345]: 328 $[M+H]^+$; 310 $[M+H-H_2O]^+$; 284 $[M+H-CO_2]^+$; 282 $[M+H-NO_2]^+$ | |
| Aristolactam Ia O-sulfate (**7**) | 359 | 20.9 | 264, 277, 292, 328, 344, 379, 396 | | 358 $[M-H]^-$<br>$MS^2$ [358]: 278 $[M-H-SO_3]^-$ |
| Aristolochic acid I (**1**) | 341 | 24.9 | 250, 320, 393 | 359 $[M+NH_4]^+$;364 $[M+Na]^+$; 700 $[2M+NH_4]^+$; 705 $[2M+Na]^+$<br>$MS^2$ [359]: 342 $[M+H]^-$; 298 $[M+H-CO_2]^+$; 296 $[M+H-NO_2]^+$ | |
| Aristolactam Ia (**4**) | 279 | 30.1 | 243, 259, 294, 332, 399 | 280 $[M+H]^+$<br>$MS^2$ [280]: 250 $[M+H-H_2CO]^+$; 225 $[M+H-CO-HCN]^+$ | |
| Aristolactam I (**3**) | 293 | 42.3 | 239, 259, 298, 329 395 | 294 $[M+H]^+$<br>$MS^2$ [294]: 279 $[M+H-CH_3{\cdot}]^+$; 251 $[M+H-CH_3{\cdot}-CO]^+$ | |

## Table 2

IPK experiments. Renal excretion parameters of unmetabolized aristolochic acid I. Individual results for Kidney A and Kidney B for 50 μM dose.

| | Kidney A | Kidney B |
|---|---|---|
| Urine flow rate (mL/min)[a] | 0.0756 (0.0126) | 0.0742 (0.0133) |
| GFR (mL/min)[a] | 0.650 (0.064) | 0.612 (0.069) |
| $CL_R$ (mL/min)[b] | 0.00142 | 0.00357 |
| $CL_{FILT}$ (mL/min)[c] | 0.0146 | 0.0138 |
| XR[d] | 0.10 | 0.26 |
| Cumulative excretion (% dose)[f] | 0.063 | 0.162 |
| Kidney accumulation (% dose)[g] | 68 | 53 |

[a] Data reported as mean (S.D.) of the seven first collection periods (10–80 min).

[b] Renal clearance calculated as ratio of cumulative urinary excretion and AUC from 0 to 80 min post-dose.

[c] Filtration clearance = GFR × $f_u$. Fraction of AA-I unbound in perfusate ($f_u$) was 0.0225.

[d] Excretion ratio = $CL_R/CL_{FILT}$.

[f] Cumulative urinary excretion (expressed as % administered dose) at 80 min post-dose.

[g] Kidney accumulation (expressed as % administered dose) at 80 min post-dose.

**Table 3**

Concentrations (μM) of AA-I and the metabolites at the 70–80 min period in perfusates and urines collected from isolated kidneys A and B perfused with 50 μM AA-I and the urine of rats (24 hr collection) subcutaneously injected with AA-I (2 mg) (Standard Deviation in parentheses).

| | IPK experiments | | | | Subcutaneously injected rats |
|---|---|---|---|---|---|
| | Kidney A | | Kidney B | | |
| **Compound** | **Perfusate** | **Urine** | **Perfusate** | **Urine** | **Urine** |
| AA-I (**1**) | 16.07 | 0.48 | 23.8 | 0.94 | 0.20 (0.05) |
| AA-Ia (**2**) | 1.24 | 0.68 | 0.42 | 4.38 | 24.1 (4.0) |
| L-I (**3**) | 0.002 | 0.053 | 0.018 | 0.055 | 0.018 (0.013) |
| L-Ia (**4**) | 0.010 | 0.16 | 0.024 | non-determined | 5.76 (2.43) |
| AA-Ia-O-S (**5**) | nd | 0.36 | nd | 0.74 | nd/traces |
| L-Ia-O-G (**6**) | nd | 0.031 | 0.014 | 0.021 | 0.15 (0.12) |
| L-Ia-O-S (**7**) | nd | nd | nd | nd | 0.15 (0.07) |

nd: non-detected

## Table 4

IPK experiments. Average excretion ratios (XR) for AA-I (**1**) and the metabolites AA-Ia (**2**), L-Ia (**4**) and L-I (**3**).

| | Kidney A | Kidney B |
|---|---|---|
| AA-I (**1**) | 0.14 (0.05) | 0.24 (0.05) |
| AA-Ia (**2**) | 12 (10) | 130 (77) |
| L-Ia (**4**) | 62 (50) | 160 (131) |
| L-I (**3**) | 130 (85) | 33 (22) |

Data reported as mean (S.D. in parenthesis) representing 7 collection periods (10–20, 20–30, 30–40, 40–50, 50–60, 60–70 and 70–80 min) per perfusion experiment.
The metabolites AA-Ia-O-S (**5**) and L-Ia-O-G (**6**) were only secreted to the urine.
L-Ia-O-S (**7**) could not be detected in the IPK experiments.